Structural properties of GaAs oxide layers grown on polished (100) surfaces

1993 J. Phys.: Condens. Matter 5 1229

(http://iopscience.iop.org/0953-8984/5/9/008)

J. Phys.: Condens. Matter 5 (1993) 1229–1238. Printed in the UK

Structural properties of GaAs oxide layers grown on polished ⟨100⟩ surfaces

M G Proietti†, J García†, J Chaboy‡, F Morier-Genoud§ and D Martin§

† Instituto de Ciencia de Materiales de Aragon, Consejo Superior de Investigaciones Cientificas, Universidad de Zaragoza, Plaza San Francisco, 50009 Zaragoza, Spain
‡ INFN, Laboratori Nazionali di Frascati, POB 13, 00044 Frascati, Italy
§ Ecole Politechnique Federale de Lausanne, CH 1015, Lausanne, Switzerland

Received 29 September 1992, in final form 4 January 1993

Abstract. The local structure of GaAs oxides, grown on GaAs ⟨100⟩ wafers by simple exposure to air after chemical etching as well as by heating in air at 250 °C and at room temperature in ozone (O_3) atmosphere, has been studied by glancing-angle x-ray absorption spectroscopy. The reflection geometry makes it possible to collect the EXAFS (extended x-ray absorption fine-structure) signal related to a thin surface layer (about 30 Å) in such a way as to reduce the unwanted substrate contribution and to collect the signal arising from the oxide grown at the surface. The oxide composition and thickness change as the surface varies from about 5 to 30 Å. An As-enriched oxide is produced by the 30′ O_3 exposure while the Ga oxide component is more abundant for the sample heated at 250 °C in air.

1. Introduction

GaAs oxides have been extensively studied [1–4] due to their importance in the epitaxial growth of III–V compounds as well as in device fabrication technology.

A 'sacrificial' oxide layer can be used, for example, to passivate and preserve a clean GaAs surface before the MBE growth. On the other hand the GaAs oxidation process is quite complex, with the Ga and As atoms reacting in a different way to oxygen exposure and with As_2O_3 desorbing at lower temperatures than Ga_2O_3.

Thin oxide layers are often grown on GaAs by simply heating the wafers after chemical cleaning. An extensive study has been published [5] on the morphology of thermal oxides as a function of the oxidation time showing the presence of amorphous and crystalline Ga_2O_3, $GaAsO_4$ and pyramidal clusters of crystalline As for oxidation states of the surface higher than ours (15′ at 500 °C).

Among the various techniques of cleaning and passivating GaAs surfaces, exposure to an O_3-rich atmosphere has become quite popular during recent years [6, 7]. The cleaning action occurs through a complex reaction involving UV photons, atmospheric oxygen and C atoms chemisorbed on the surface. The UV wavelengths of interest are 184.9 and 253.7 nm. The first wavelength is absorbed by the oxygen, producing O_3 that reacts with the C atoms of the surface forming volatile CO_2. In such a way carbon contamination, which is responsible for defect generation on the surface of the epitaxial overlayers, and the consequent degradation of the material properties, is strongly reduced. The 253.7 nm UV wavelength, on the other hand, being absorbed by

O_3, leads to the formation of O_2 and atomic oxygen, which is a very strong oxidation agent.

The O_3 oxides seem to have a different composition from native and thermal oxides and to leave, when desorbing in ultra-high vacuum, a more stoichiometric GaAs surface.

Few XPS studies have been published on the subject [8–10] and, to our knowledge, only one [11] concerns the direct determination, by means of EXAFS, of the structural parameters of native GaAs oxide.

The aim of this work is therefore to provide a microscopical picture of the local atomic structure of O_3 oxides by means of glancing-angle EXAFS and to compare it with the structure of thermal and native oxides. A near-surface study can be carried out due to the low x-ray penetration depth for glancing angles lower than the critical angle for which the system undergoes the total reflection regime [12].

2. Experimental details

The samples have been prepared using two-inch diameter LEC grown polished (100)-oriented GaAs wafers supplied by Sumitomo Corp. A typical chemical cleaning recipe suitable for MBE wafer preparation was used before the thermal O_3 treatment. The UV/O_3 treatment has been carried out in a UV lamp box containing air, in a clean room. The sample was placed on a rotating sample holder, mounted at a distance of about 1 mm from a 10 W low-pressure Hg lamp with a quartz bulb. The temperature of the sample surface during the treatment was about 90 °C. The following set of five samples was prepared.

(1) A polished wafer etched with H_2SO_4, rinsed with deionized (DI) water, heated at 250 °C for 30 s, etched with HCl, rinsed with DI water and heated again for 30 s.

(2) A polished wafer etched with H_2SO_4, rinsed with DI water and heated in air at 250 °C for 10 min.

(3) A polished wafer, H_2SO_4 etched, rinsed with DI water, HCl etched, rinsed with DI water, exposed to a UV lamp under oxygen flux for 2 min.

(4) As above but exposed to O_3 for 10 min.

(5) As above but exposed to O_3 for 30 min.

The absorption spectra were taken, at room temperature, detecting the fluorescence signal at the Ga and As K edges, in the glancing-angle geometry at station 9.3 of the Daresbury synchrotron radiation source.

A double Si(220) crystal monochromator has been used for the whole set of measurements and the rejection of higher-order reflection was achieved by slightly detuning the Si crystals from the parallel alignment. The incident beam was collimated by a 50 μm precision slit and the horizontal zero position of the sample was determined using a second 50 mm slit with a precision better than 5 m°. The incident and reflected intensities were detected by ionization chambers while the fluorescence signal was monitored by an array of 13 individual 11 mm diameter Ge detectors working at liquid nitrogen (LN) temperature. The use of such an SSD system allows both good background filtering and the elimination of the elements affected by Bragg diffraction peaks, the individual signals being recorded separately.

The measurements were performed in the total reflection regime, i.e. at incidence angles ϕ below the critical angle ϕ_c, evaluated by measuring the reflectivity curve at a fixed energy, above the absorption edge, for each sample.

The ratio ϕ/ϕ_c has been chosen equal to 0.5 to get a good trade-off between the quality of the EXAFS signal and the distortion introduced in the spectrum by the energy dependence of the reflectivity [13]. The penetration depth is estimated to be about 30 Å [14]. A typical reflectivity curve is shown in figure 1.

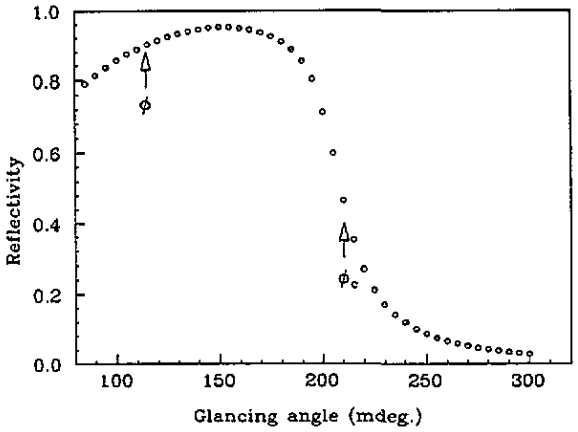

Figure 1. Reflectivity as a function of the incidence angle, for sample 1 at E = 10.2 keV. The arrows indicate the reflectivity at the critical angle, ϕ_c, and at the angle of measurement ϕ.

3. Results and discussion

The EXAFS signals have been extracted from the raw absorption spectra using standard methods [15] and are shown, for the whole set of samples, in figure 2 for the As K edge. The EXAFS signal for a powdered sample of crystalline GaAs, measured in the standard transmission mode, is given in figure 2(*f*) for comparison.

As we can observe the EXAFS signal is clearly GaAs-like for samples 1, 2, 3 and 4. For sample 5, it has instead the typical shape due to oxygen backscattering function, indicating an increased oxide thickness and a correspondent decrease of the GaAs bulk contribution. The oxide contribution is much less apparent in samples 2 and 3 due to the low oxide thicknesses and a careful fit procedure is needed. In any case the bulk GaAs contribution is always present in the glancing-angle spectra even in the case of the thickest oxide layer (sample 5). This means that the beam always reaches the GaAs substrate and that the thickness of the oxide layer is lower than the estimated penetration depth of about 30 Å. The same considerations apply to the Ga K-edge spectra.

The EXAFS spectra of samples 1, 2 and 5, at both Ga and As K edges, have been analysed by means of a theoretical fitting procedure in order to give a deeper insight. Theoretical phases and amplitudes have been generated by the program FEFF [16], and tested on GaAs. The transmission spectrum of figure 2(*f*) has been used as a reference and values very close to the crystallographic ones have been obtained. The results of the best fit are shown in figure 3 for the As K edge and the corresponding values of the fit parameters are reported in table 1.

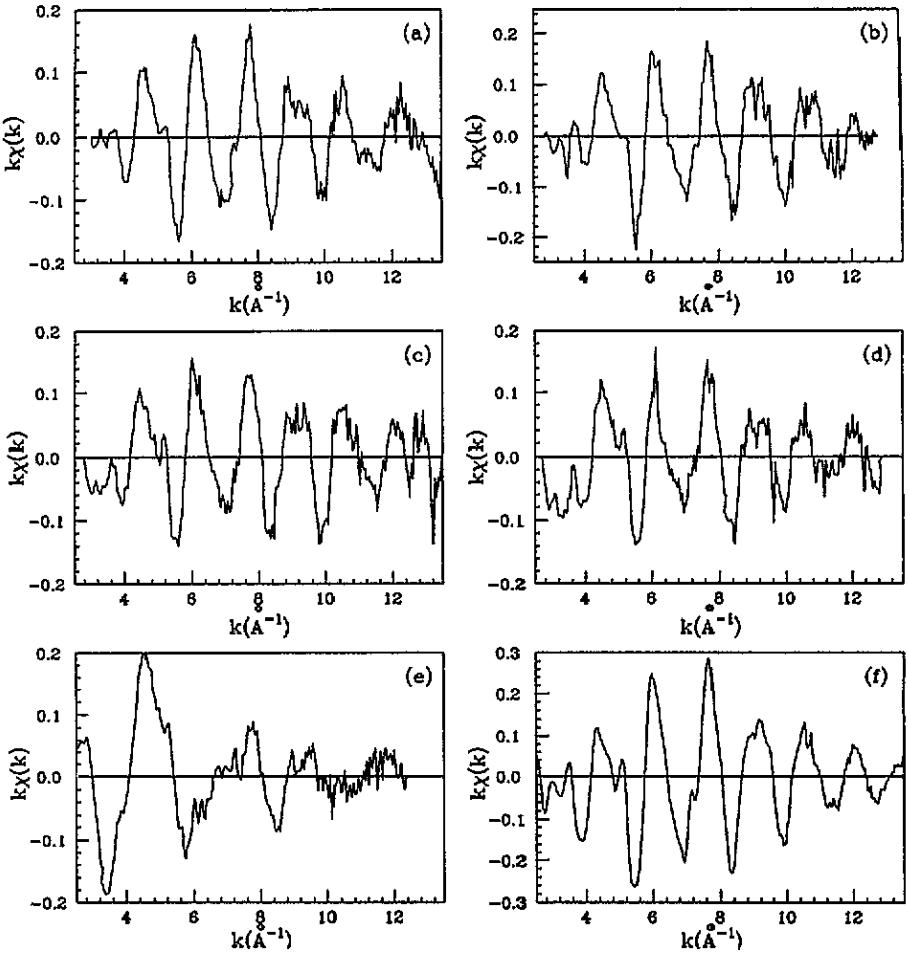

Figure 2. Raw k-weighted EXAFS signals for samples 1(*a*), 2(*b*), 3(*c*), 4(*d*) and 5(*e*) and for GaAs at 77 K in standard transmission mode (*f*), at the As K edge.

The program NPI [17], based on an iterative least-square fitting procedure, has been used to refine the theoretical values according to the following procedures.

As a first step, the first peak of the Fourier transform (FT) of the EXAFS spectra was Fourier filtered and a best fit was carried out starting from the crystallographic values of the Ga–As, As–O and Ga–O distances in bulk GaAs, As_2O_3 and Ga_2O_3 respectively. Then the Fourier filtering was extended up to about 3 Å to include in the EXAFS signal to be fitted the second-peak contribution due to the second GaAs coordination shell and to the Ga–O–Ga(As) and As–O–As(Ga) coordination shells of the oxide layer. The second-shell parameters were iterated starting from the expected crystallographic values and a little further refinement of the first-shell distance was allowed. As a last step, the R-space spectra were antitransformed extending the transformation interval up to about 5 Å, i.e. including the GaAs third-shell contribution.

The results of the best fits are summarized in table 1 and the Fourier-filtered

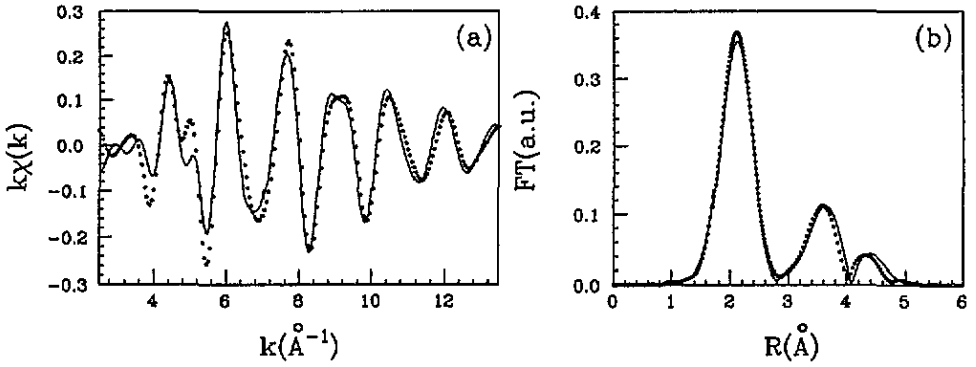

Figure 3. As K edge calculated (full curve) and experimental (dotted curve) k-weighted filtered EXAFS signals (*a*) with the corresponding Fourier transforms (*b*) for crystalline GaAs. The spectrum was taken at room temperature in transmission mode, from a powdered sample.

EXAFS spectra with the correspondent FT are shown in figures 4 and 5 for the As and Ga K edges respectively, together with the best-fit theoretical curves.

As mentioned before, the zinc-blende environment, typical of bulk GaAs, is always observed, even for the thickest oxide layer. The interatomic distances as well as the nearest-neighbours (NN) coordination numbers are in good agreement with the typical values for GaAs (see table 3). The next-nearest-neighbour (NNN) coordination values are however in poor agreement with the expected values. This may be due to an amplitude distortion effect related to the glancing-angle technique, and is presently under further investigation. Therefore the second- and third-shell analysis reported here is qualitative and it will be taken into account only to confirm the results obtained from the lower coordination shells.

In the case of sample 1, i.e. the native oxide obtained by simple air exposure after chemical cleaning, a distance of 1.7 Å is observed in the spectrum at the As K edge while the corresponding Ga spectrum exhibits a Ga–O bondlength of about 2 Å.

The crystallographic parameters of the various Ga and As oxides that have been considered as possible components of the samples under study are summarized in table 2. The As–O bondlength is consistent both with the presence of cubic (arsenolite) [18] and monoclinic (claudetite) [19] forms of As_2O_3. The Ga environment is characterized by a further Ga–Ga shell at about 3.5 Å, observed also for the other samples, which points to the presence of distorted octahedral Ga_2O_3 whose Ga–O bondlength is between 1.9 and 2.1 Å with octahedra connected together through a Ga–O–Ga bond [20].

The NN coordination numbers are very low, indicating that the oxide layer is quite thin. A rough estimate of the oxide layer thickness can be made by considering the relative intensities of the oxide and bulk contributions with respect to the expected x-ray penetration depth of about 30 Å. An overall thickness not larger than 5 Å is deduced for sample 1. This is a little less than the values deduced by other authors [11], but in that case the sample studied was a GaAs wafer as received from the vendor and not an etched and freshly oxidized sample as in our case.

The thermal oxide, i.e. sample 2, shows an increased Ga-oxide component and a shoulder on the low-R side of the first FT peak appears, corresponding to an

Table 1. Shell distance R (Å), coordination numbers N, and Debye–Waller factors $2\sigma^2$ (Å^2) obtained from least-squares fitting of filtered EXAFS data. M stands for As and/or Ga.

	As K edge						Ga K edge					
	As–O			As–O–M			Ga–O			Ga–O–M		
Sample	R	N	σ^2	R	N	σ^2	R	N	σ^2	R	N	σ^2
1	1.7	0.5	0.006	—	—	—	1.99	0.4	0.006	3.56	0.75	0.012
2	1.7	0.4	0.006	3.1	0.75	0.010	1.96	0.8	0.008	3.6	1.1	0.012
5	1.7	3.75	0.006	2.8	2	0.013	1.80	0.37	0.006	3.6	1.1	0.012
				3.12	1.1	0.012	2.01	1.4	0.006			

	As K edge									Ga K edge								
	As–Ga			As–As			As–Ga			Ga–As			Ga–Ga			Ga–As		
Sample	R	N	σ^2	R	N	σ^2	R	N	σ^2	R	N	σ^2	R	N	σ^2	R	N	σ^2
1	2.448	3.8	0.006	3.95	5	0.013	4.65	1.5	0.015	2.448	3	0.006	4	1.8	0.015	4.63	2.5	0.015
2	2.448	3.8	0.005	3.97	4	0.015	4.62	2	0.015	2.448	2.4	0.006	4	0.75	0.012	4.67	0.75	0.012
5	2.448	1	0.006	3.97	1.6	0.01	4.65	1	0.016	2.448	1.2	0.006	—	—	—	—	—	—
GaAs	2.446	4.2	0.003	3.99	12	0.009	4.67	12	0.014	2.448	4	0.003	3.99	12	0.010	4.68	12	0.015
Transmission																		

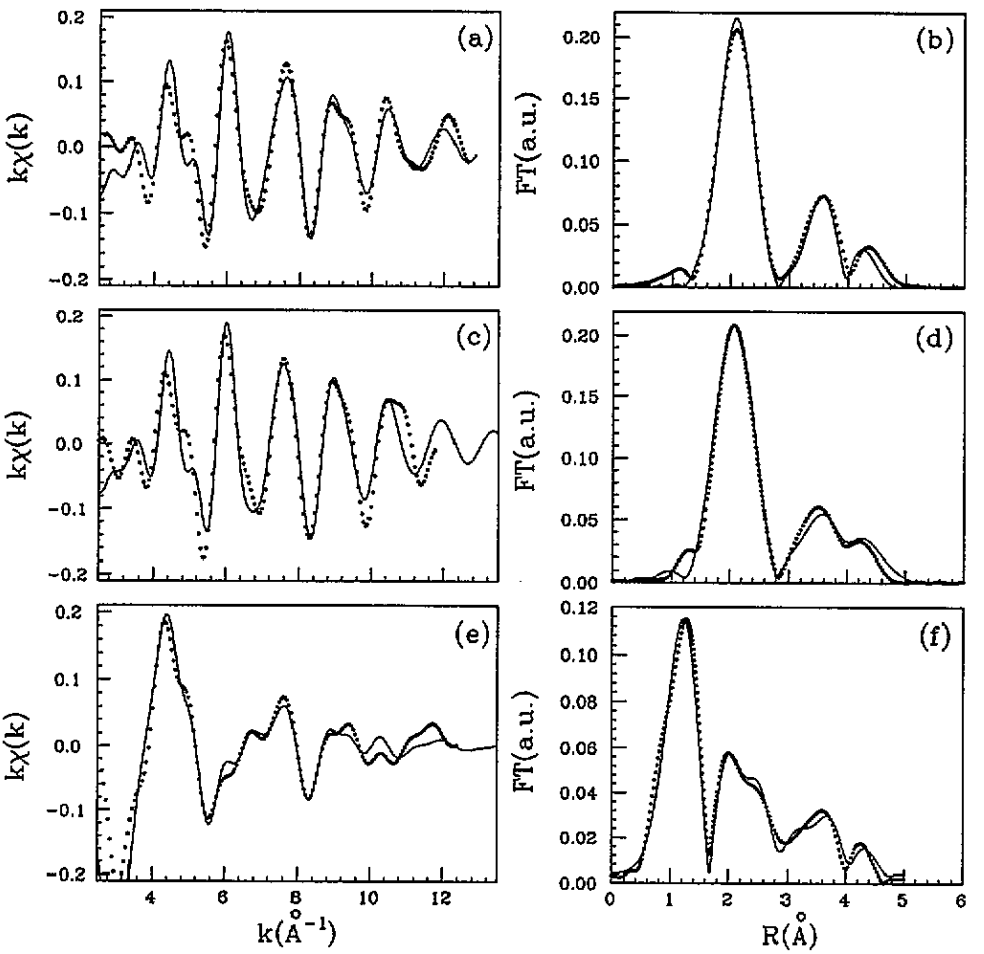

Figure 4. As K edge calculated (full curve) and experimental (dotted curve) k-weighted filtered EXAFS signals with the corresponding Fourier transforms for sample 1(*a*,*b*), 2(*c*,*d*) and 3(*d*,*e*).

increase in the coordination number of the Ga–O correlation shell. A corresponding decrease in the NN coordination of the zinc-blende structure is observed, confirming the increasing oxide layer thickness. This change in the composition is due to the different heats of formation of As_2O_3 and Ga_2O_3, which favour the growth of Ga oxides, and has been already observed by XPS [10]. Moreover, As tends to desorb as the temperature increases, leaving an As-depleted surface. For the As oxide, distances and coordination numbers of the As–O shell from sample 2 are similar to sample 1, while a further coordination shell, related to an As–O–As correlation, appears at about 3.1 Å. This is in agreement with the NNN distance predicted for As_2O_3 in the claudetite phase [19] and points to the presence of a more homogeneous oxide layer produced by heating. The overall estimated oxide thickness is of about 10 Å.

A more evident change is observed for the sample oxidized for 30 min in the O_3/UV atmosphere. The FT peaks corresponding to the As–O and Ga–O correlations are now apparent and resolved from the GaAs peaks which are in turn strongly

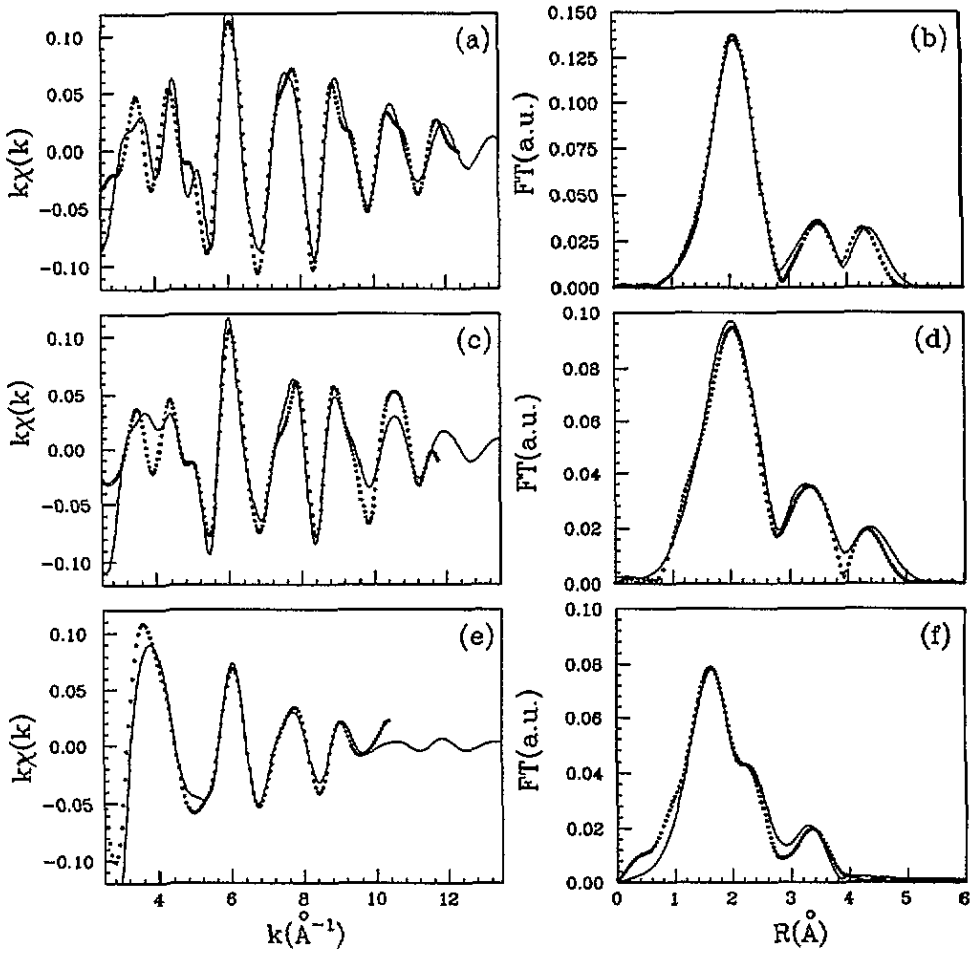

Figure 5. Ga K edge calculated (full curve) and experimental (dotted curve) k-weighted filtered EXAFS signals with the corresponding Fourier transforms for sample 1(*a,b*), 2(*c,d*) and 3(*e,f*).

Table 2. Crystallographic coordination numbers N and shell distances R (Å) for some As and Ga oxides.

	Ga–O		As–O		Ga–Ga		Ga–As		As–As	
Material	N	r	N	r	N	r	N	r	N	r
$GaAsO_4$	4	1.77	4	1.72			4	3.16		
α-Ga_2O_3	3	1.92			1	2.83				
	3	2.08			3	2.94				
					3	3.31				
					3	3.64				
As_2O_3[a]			3	1.79					3	3.22
As_2O_3[b]			3	1.80					3	3.17

[a] Arsenolite phase of As_2O_3 [18].
[b] Claudetite phase of As_2O_2 [19].

Table 3. Crystallographic coordination numbers N and shell distances R (Å) for GaAs.

L	N	r
LGa–As	4	2.45
LGa–Ga	12	3.97
LGa–As	12	3.17

reduced. The total oxide thickness is estimated to be about 25–30 Å, since the oxide contribution to the first FT peak dominates the GaAs contribution. Moreover, the Ga and As environments are clearly different. The As oxide is in this case more abundant than the Ga oxide, as deduced by the relative intensities of the corresponding FT peaks. The fit results indicate the same As–O distance as for samples 1 and 2, with a strong increase of the corresponding coordination number, while for the As–O–As correlation two different distances are found: 3.13 and 2.8 Å. The first one is the same as in the thermal oxide while the second is not predicted by any stable phase of As_2O_3. This latter value of distance has been observed by other authors in native GaAs oxides [12] and explained in terms of oxygen atoms entering in the GaAs structure in substitutional sites and bridging As and/or Ga atoms. This would result in a contraction of the NNN distance of GaAs corresponding to a bond angle of about 107°, i.e. still close to the zinc-blende tetrahedral angle.

At the Ga K edge a further Ga–O distance is observed at 1.8 Å together with the previous one at 2 Å. It could be attributed to the Ga–O bondlength in the distorted octahedron characteristic of the monoclinic β-Ga_2O_3 [21] as well as to the presence of $GaAsO_4$. This oxide mixed phase is characterized by NN Ga–O and As–O distances of 1.77 and 1.72 Å [22] and the NN coordination number is four for both Ga and As. It could be predicted, together with Ga_2O_3, in the reordering process of an amorphous mixture of As_2O_3 and Ga_2O_3 that is expected to be metastable [19]. Furthermore it has been observed also in thermal GaAs oxides grown at temperatures around 500 °C for at least 15 min, i.e. in samples with oxidation levels higher than in our study [5]. The presence of $GaAsO_4$ is also in agreement with the As–O coordination number higher than three, the value expected for As_2O_3, found for this sample.

As a last remark we can briefly comment, in a qualitative way only, the results obtained for samples 3 and 4 treated with O_3 for 2 min and 10 min respectively. After the first 2 min the oxide amount is still very low, comparable with the native 'fresh' oxide. Changes in the oxide layer, surface stoichiometry and desorption mechanisms have been observed in previous XPS studies [23] but it is quite different to extract reliable information by an EXAFS analysis due to the very low oxide thickness.

After a 10 min treatment an increase in the Ga component of the oxide seems to occur. This would point to some enrichment of Ga at the surface, as observed by XPS for air oxidized samples [24], but in contrast with XPS results from other authors on UV/O_3 oxides [8]. Such disagreement could be attributed to some difference in the growth process. In that case the oxide was indeed grown *in situ* under a controlled oxygen flux.

4. Conclusions

We studied the oxidation process of GaAs(100) surfaces by glancing-angle x-ray absorption spectroscopy. Native, thermal and O_3/UV oxides have been compared.

The results show that the oxide composition and thickness change with the sample treatment.

The native oxide has a thickness of about 5 Å and is composed of a mixture of approximately equal amounts of Ga and As oxides, probably non-stoichiometric and amorphous with the local configuration of arsenolite and/or claudetite for As and of β-Ga_2O_3 for the Ga oxidation state. The presence of $GaAsO_4$ seems to be ruled out due to the absence of the corresponding Ga–O distance in the Ga K-edge spectrum.

The thermal oxide shows an increased thickness related to an increased Ga oxide amount, as expected from its lower heat of formation.

The most remarkable changes, with respect to the native oxide, are observed in the 30 min O_3 treated sample: the oxide thickness is about 25 Å and the amount of the As oxide component is greater than the Ga oxide one, showing that the As oxidation process is made favourable by O_3. The presence of the $GaAsO_4$ is observed as a likely consequence of some crystallization and re-ordering of the oxide layer.

Acknowledgments

The authors wish to thank Dr Andy Dent and Dr Barry Dobson of SERC Daresbury for their helpful and kind assistance during the measurements. This work has been partially supported by the CICYT project MAT90-0734.

References

[1] Pianetta P, Lindau I, Garner C M and Spicer W E 1978 *Phys. Rev.* B **18** 2972
[2] Su C Y, Lindau I, Cheye P W, Skeath P R and Spicer W E 1982 *Phys. Rev.* B **25** 4045
[3] Landgren G, Ludeke R, Morar J F, Jugnet Y and Himpsel F J 1984 *Phys. Rev.* B **30** 4839
[4] Bartels F and Monch W 1984 *Surf. Sci.* **143** 315
[5] Schwarz S A, Hwang D M and Chen C Y 1990 *Phys. Rev.* B **44** 3025
[6] Rao V B and Koyama R Y 1984 *J. Electrochem. Soc.* **131** 1674
[7] Vig J R 1985 *J. Vac. Sci. Technol.* A**3** 1027
[8] Cossu G, Ingo G M, Mattogno G, Padeletti G and Proietti M G 1992 *Appl. Surf. Sci.* **56** 81
[9] Flinn B J and McIntyre N S 1990 *Surf. Interface Anal.* **15** 19
[10] Ingrey S I J, Lau W M and Sohdi R N S 1989 *J. Vac. Sci. Technol.* A**7** 1554
[11] Barret N T, Greaves G N, Pizzini S and Roberts K J 1990 *Surf. Sci.* **22** 337
[12] Heald S M, Chen H and Tranquada J M 1988 *Phys. Rev.* B **38** 1016
[13] Martens G and Rabe P 1980 *Phys. Status Solidi* a **58** 415
[14] Parrat L G 1954 *Phys. Rev.* **95** 2
[15] 1986 *X-Ray Absorption: Principles, Application, Techniques of EXAFS, SEXAFS and XANES* ed D C Konigsberger and R Prins (New York: Wiley) ch I–VI
[16] Rehr J J, Mustre de Leon J, Zabinsky S I and Albers R C 1991 *J. Am. Chem. Soc.* **113** 5137
Rehr J J and Zabinsky S I 1991 *Phys. Rev.* B **44** 4146
Rehr J J, Albers R C and Mustre de Leon J 1989 *Physica* B **158** 417
[17] NPI Sanchez del Rio M and Chaboy J 1991 Program NPI *European Synchrotron Radiation Facility, Internal Report* EXP/MSR/91/12
[18] Pertlik F 1975 *Monats. Chem.* **106** 755
[19] Pertlik F 1978 *Czechoslovak J. Phys.* **28** 170
[20] Marezio M and Remeira J P 1960 *J. Chem. Phys.* **46** 1862
[21] Geller S 1960 *J. Chem. Phys.* **33** 676
[22] Schwartz B 1975 *CRC Crit. Rev. Solid State Sci.* **5** 609
[23] Goiffon A, Bayle G, Astier R, Jumas J C, Maurin M, Philippot E 1983 *Rev. Chim. Mineral.* **20** 338
[24] Iwasaki H, Mizokawa Y, Nishitani R and Nakamura S 1979 *Surf. Sci.* **86** 811